

Silicon nanophotonic waveguides and their applications

Wim Bogaerts, Liu Liu, Shankar Kumar Selvaraja, Pieter Dumon, Joost Brouckaert, Dirk Taillaert, Diedrik Vermeulen, Gunther Roelkens, Dries Van Thourhout and Roel Baets

Ghent University - Interuniversity Microelectronics Centre (IMEC), Department of Information Technology (INTEC), Sint-Pietersnieuwstraat 41, 9000 Gent, Belgium

ABSTRACT

We discuss silicon photonic wires and components based on this technology, such as filters based on ring resonators, interferometers or arrayed waveguide gratings. The devices are fabricated using standard CMOS technology, including 193nm lithography. We also discuss their application in a number of demonstrator devices within different application fields.

Keywords: silicon photonics, nanophotonics, photonic wire, ring resonator, arrayed waveguide grating, optical filter

1. INTRODUCTION

In the last decade, silicon photonics has gained substantial importance in the field of photonic integration. This is because of the combination of a very high index contrast (and thus strong miniaturization) and the compatibility with CMOS fabrication technology.¹

Silicon nanophotonic waveguides, often called photonic wires, can strongly confine light in a submicron waveguide core, allowing sharp bends and compact components. This allows for a dramatic reduction in footprint, which in turn enables larger-scale integration of photonic components.¹ Because of the high index and sharp bends, elementary building blocks, such as splitters, ring resonators, and even all-out demultiplexers based on arrayed waveguide gratings can be made more compact.² This is helped even more by the relatively high group index of photonic wires.³

The attractiveness of silicon photonic wires not only comes from the small scale of the waveguides, but also from the possibility of leveraging the industrial fabrication base of electronics. The fabrication of photonic wires and many other components can be done with the same tools made for making transistors.^{1,4} In section 2 we show how industrial tools are used to fabricate high-quality silicon photonic wire circuits.

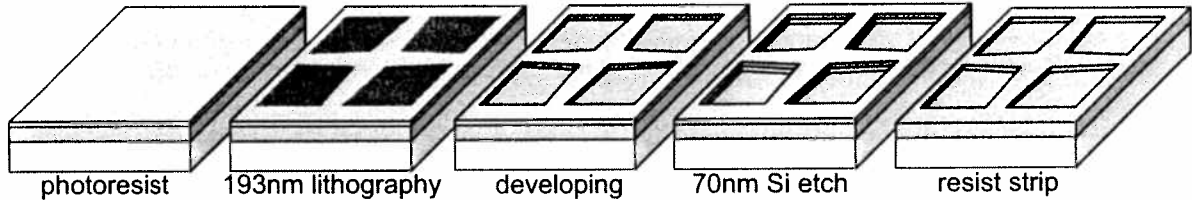
In section 3 we discuss the performance metrics of photonic wire waveguides and show that the losses are sufficiently low to make relatively large integrated circuits. However, while photonic wires offer superb performance in terms of mode confinement and bend radius, the high refractive index contrast can work adversely where it can introduce unwanted scattering at abrupt interfaces. Therefore, we have introduced a two-level etch scheme: we define both high-contrast wires in a deep etch step, and lower-contrast rib structures in a shallow etch.^{2,5} These rib structures are used in situations where the high contrast is not desirable. In addition, the shallow etch also serves a different purpose: the definition of diffractive gratings which can be used for incoupling and outcoupling.

In section 4 we present the most recent result for a variety of wavelength selective devices based on this technology: ring resonators, arrayed waveguide gratings, planar concave gratings, splitters, waveguide crossings (especially hard to do in high-contrast materials). Also, in section 4.4 we will address the problem of interfacing a submicron high-contrast waveguide with a standard optical fiber.

We will also discuss a number of possible applications where this technology could have unique advantages: communications (especially datacom and access/metro networks), sensing (environment, structural monitoring) and health-care (diagnostic tools). In section 5 we will discuss three case studies where silicon photonics could be used to scale down a device dramatically.

Further author information: (Send correspondence to W.B.)
W.B.: E-mail: wim.bogaerts@intec.ugent.be, Telephone: 32 9 264 3324

Shallow-etched regions (gratings, intersections, rib waveguides, ...)



deep-etched regions (photonic wires, echelle facets, ...)

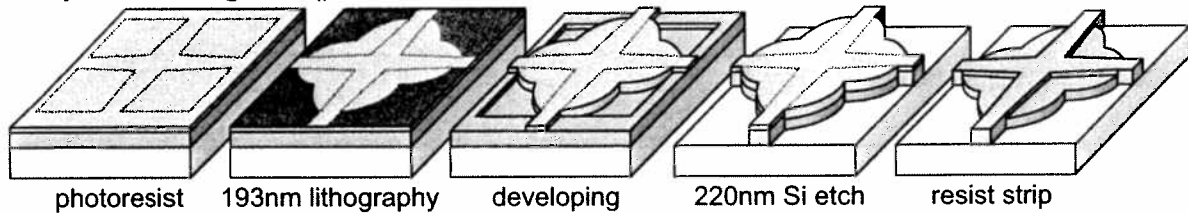


Figure 1. Fabrication process for passive silicon nanophotonic waveguide components. Two etch layers are used. First, as shallow etch layer is patterned, which contains diffraction grating couplers and low-contrast rib waveguides. After that, the deep-etched regions, such as the waveguide trenches, are defined.

2. FABRICATION TECHNOLOGY

The use of silicon for photonic integrated circuits makes it compatible with CMOS processes in terms of materials. This only implies that photonics could be made in the same tools without issues of contamination. However, the requirements in terms of feature size and layer thickness are quite different than those for electronics.

The devices shown here in this paper are fabricated using the CMOS research facilities of IMEC, Belgium, using industrial 200 mm tools compatible with a 130 nm CMOS technology node. We use SOITEC Smartcut wafers with a buried oxide of 2 μm thick and a top silicon layer of 220 nm. The fabrication process is illustrated in figure 1. A mask pattern is defined using 193 nm optical projection lithography. After baking and developing, the pattern is transferred into the silicon using an ICP-RIE etch. Finally, the resist is stripped.^{1,6}

Photonic wires require a strong lateral index contrast to allow for sharp bends. However, for some other elements a lower contrast is preferred. To combine high contrast waveguides with a local lower contrast, we use two etch layers. First, shallow etch regions (70 nm etch depth) are defined, followed by the deeply etched waveguide trenches. This dual-contrast approach has many benefits, and enables very compact devices without some of the penalties that come with very high contrast waveguides. The use of high-end CMOS tools allows very accurate alignment at wafer scale, with alignment tolerances of the order of 10 nm.

Nanophotonic waveguides, and especially wavelength-selective elements put much more stringent demands in terms of process control. Where process windows in CMOS devices are typically of the order of 5-10% of the critical dimensions, the uniformity of photonic wires should be controlled within 1%, and preferably within 1 nm. In a ring resonator, discussed in section 4, a 1 nm change in width will typically result in a corresponding shift in resonance wavelength. We have demonstrated that this level of control is possible on standard tools for CMOS fabrication.⁶

3. NANOPHOTONIC SILICON WAVEGUIDES

3.1 Photonic wires

The high refractive index contrast of silicon ($n = 3.45$) with silicon dioxide ($n = 1.45$) makes it possible to confine light in a core with submicron dimensions. The core of such a waveguide is shown in figure 2.

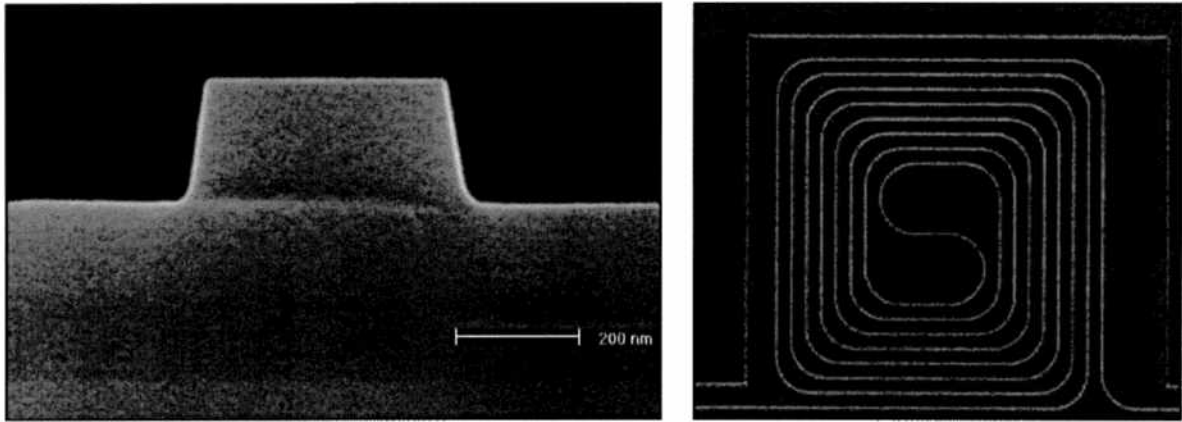


Figure 2. Photonic wire waveguide. The light is confined in the submicron silicon core, surrounded by an oxide and air cladding. Left: core cross section. Right: a spiral waveguide to characterize propagation and bend losses.

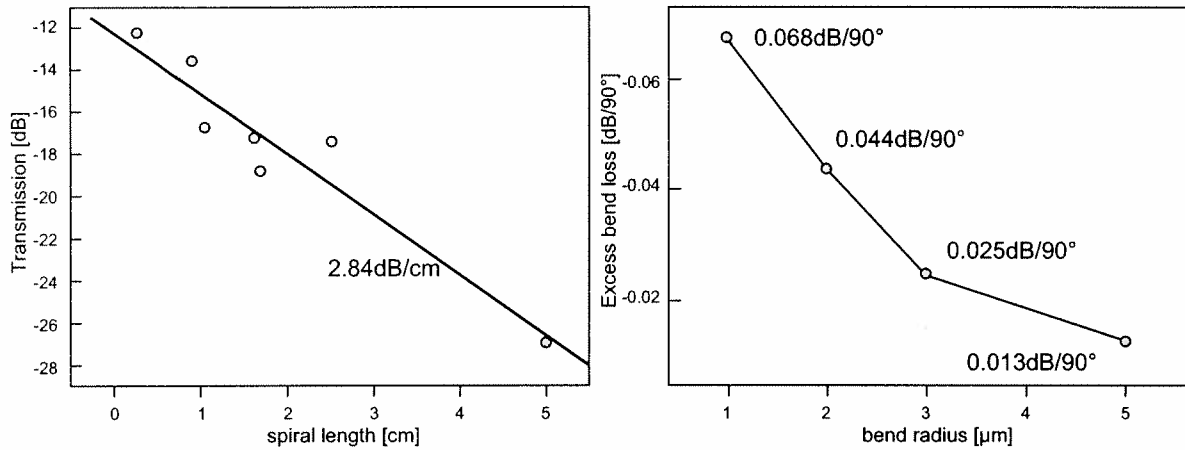


Figure 3. Losses in photonic wires, extracted from spiral waveguides as shown in figure 2 Left: propagation of straight waveguides. Right: excess loss in bends.

In a photonic circuit, the scale of integration is basically determined by the interconnecting waveguides. They should have a compact core (for dense packing), low loss (for longer distances) and small bend radius with low excess loss. The basic performance of these wires is determined by the losses of the straight waveguides, as well as the excess losses in the bends.^{2,3} These metrics, measured for our photonic wires are shown in the plot in fig. 3. For wire widths between 400 nm and 500 nm the straight losses are 2.8 dB/cm. Excess bend losses are also plotted, and depend strongly on the bend radius. We see that for a bend radius larger than 3 μm , the bend losses are becoming negligible.

The photonic wires discussed in this paper are made in crystalline silicon. However, for some applications the optical layer should be deposited on top of another substrate or device. In this case, deposited amorphous silicon layers can be used. We have also demonstrated low-loss waveguides in amorphous silicon, with propagation losses of 3.54 dB/cm, only slightly higher than the losses in the crystalline waveguides.⁷ The amorphous deposition also allows us to use different layer thickness if this is required.

Crystalline silicon has superior material properties for waveguiding: with good etching, we have demonstrated photonic wire losses of 2.8 dB/cm without the need for annealing or reflow. However, the use of crystalline silicon

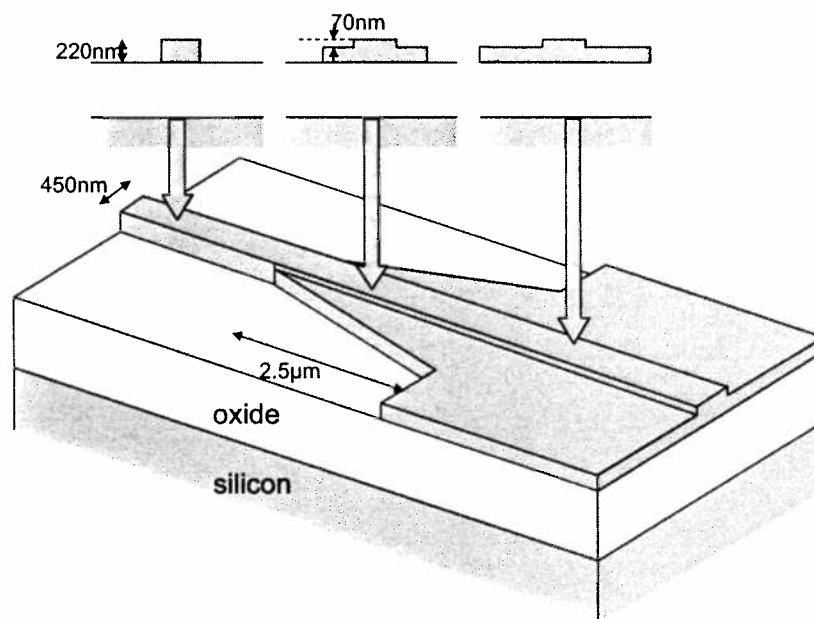


Figure 4. Transition between a photonic wire and a lower-contrast rib waveguide.

is limited to SOI substrates of specific thicknesses. Deposited silicon, on the other hand, allows for a larger flexibility.

3.2 Transition to rib waveguides

Photonic wires have a high lateral index contrast, allowing for very good confinement and small mode size. This, allows for a small footprint and sharp bends. However, this high index contrast has some disadvantages. For instance, photonic wire modes are prone to scattering losses at irregularities, or at an abrupt change in the waveguide. This can happen at waveguide intersections, or where a waveguide interfaces with a multimode interferometer (MMI) or slab regions. In such cases, a lower-contrast waveguide is preferable.

As already discussed in section 2, the waveguide contrast can be lowered by using a shallow etch instead of a deep etch. The transition between a photonic wire and a low-contrast rib can be done with a fairly simple concept, shown in figure 4. The deep-etch waveguide is expanded in width over the distance of a few microns. Over this deep etch taper, the shallow waveguide is superposed. As the deep taper expands, the shallow waveguide will take over the confinement of the light.

Note that such a shallow rib waveguide still has a relatively large refractive index contrast, compared to traditional waveguides. The effective index of the cladding slab is about 2.5, with the core slab having an effective index of 2.8.

3.3 Intersections and splitters

When going to large-scale photonic circuits, routing topology can introduce problems, as complex circuits it will require waveguide intersections. While multi-layer circuits are a option, transferring light from one circuit layer to another is not straightforward. Therefore, we optimized a high-efficiency intersection. The high refractive index contrast of a silicon photonic wire has as a consequence that a abrupt disruption of the waveguide (such as a crossing), acts as a strong scatterer, causing loss, and in the case of a crossing, substantial crosstalk. In practice, a direct crossing of a 450 nm has about 30% loss per crossing, with a -10 dB crosstalk level.

The solution to this problem is using a local lower index contrast. This is accomplished with the shallow etch described in section 2. Near the crossing, the light is transferred from a deep-etched wire to a shallow-etched

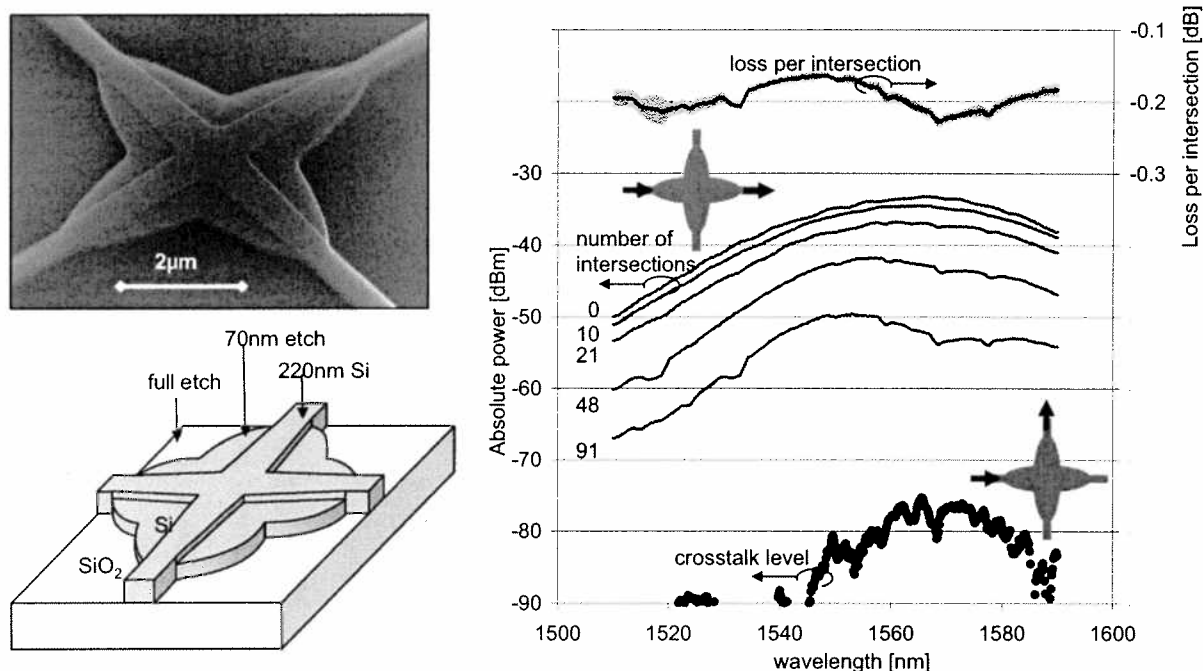


Figure 5. Low-loss waveguide crossing. Reflections and crosstalk are minimized by locally reducing the refractive index contrast with a shallow etch step. Left: SEM picture showing the two etch regions. Right: Transmission as a function of wavelength.

waveguide. The shallow-etched waveguides retains the confinement of the light, but the mode can still spread out because of the lower local contrast. In addition, correct shaping of the deep-etch region induces a phase front flattening at the crossing interface, suppressing diffraction. With this technique, crossing transmission can be increased to almost 98% (-0.15dB), with crosstalk levels of -40dB . The footprint of the crossing is $6 \times 6 \mu\text{m}^2$.

Photonic interconnections are often used for signal distribution, requiring low-loss splitters. For the same reason as with the crossing, a direct Y-splitter is not suitable, as it is difficult to fabricate the splitting point with such accuracy that it does not cause scattering. As an alternative, one can use a small multi-mode interferometer (MMI) to construct a 1×2 coupler. However, again an abrupt interface is introduced where the wire is inserted in the MMI. However, the same technique for reduction in contrast can be used. Figure 6 shows an MMI-based splitter where the interfaces between the waveguide and the MMI are implemented in a shallow-etched waveguide, with a short tapered transition between the deep and shallow waveguide. The excess loss of this splitter is of the order of -0.2dB , with an imbalance lower than 0.02dB , as measured on 50 splitters. It is also quite tolerant to fabrication variations, with fabrication errors of 100nm leading to a maximum increase of the splitter loss to only 0.20dB . The small size of the MMI also makes it quite broadband, with a nonuniformity in the transmission of 0.12dB between $1.5 \mu\text{m}$ and $1.6 \mu\text{m}$.

4. WAVELENGTH-SELECTIVE ELEMENTS

In many application, wavelength filtering is required. In telecommunication, wavelength division multiplexing (WDM) allows high-bitrate data transport on different carrier wavelengths. Also, in spectrometry, it is necessary to split light into its constituent wavelengths. Depending on the application, one can use drop filters (such as ring resonators) which separate one or a few wavelength channels, or all-out demultiplexers, such as arrayed waveguide gratings (AWG) or planar grating demultiplexers.

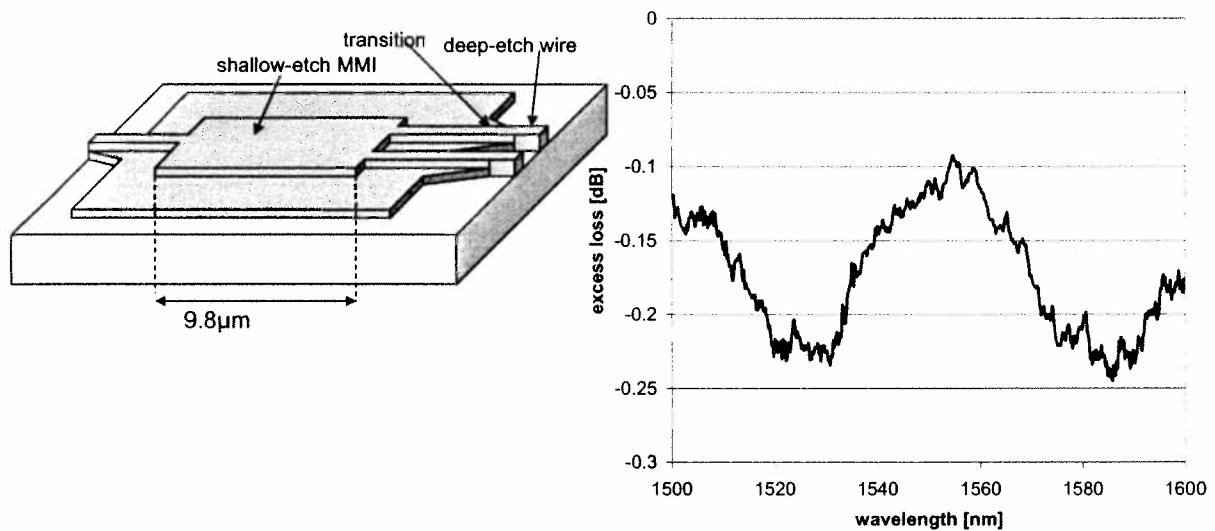


Figure 6. Photonic wire splitter based on a shallow-etched MMI. Left: the concept of a shallow MMI, Right: Measured excess loss as a function of wavelength.

In wavelength-selective waveguide components, the typical length scale depends on the group index of the waveguide used. The lower the group velocity (higher group index) of the waveguide, the shorter the physical length of the delay lines. While photonic crystals are ideally suited for such low group velocities,^{8,9} they also have higher propagation loss. Photonic wires still have a relatively high group index around 4.2, resulting in relatively short delay lines.

4.1 Ring and racetrack resonators

Ring resonators offer an extremely elegant way to separate a well-defined wavelength band from a broadband spectrum. In a ring resonator, as the one shown in figure, light resonates if the wavelength fits a whole multiple times in the circumference of the ring.^{2,3} Incoming light from the bus waveguide is coupled to the ring via a directional coupler. On resonance, light is transferred by the ring to the drop waveguide. Off resonance, light stays in the bus waveguide. The quality factor Q of the ring determines the bandwidth of dropped wavelength range, with higher Q values resulting in a narrower spectral peak. These compact ring resonators are possible in photonic wires because of the short bend radius. A compact ring allows for a large free spectral range, which allows us to use the ring over a wide spectral bandwidth.

We have demonstrated ring resonators with Q values between 10000 and 25000, and coupling efficiencies close to 100%.^{2,3,10} However, as already discussed in section 2, the rings are very sensitive to fabrication errors. Still, our fabrication process is very well controlled, giving very small deviations for nominally identical rings within the same chip, over the same wafer and even between wafers. This is shown in figure 7, where the transmission in the bus waveguide of a two identical ring notch filters 2 mm apart on the same wafer are plotted. The shift in wavelength peak is less than 1 nm.

4.2 Arrayed waveguide gratings

In an arrayed waveguide grating, the incoming light is split up in wavelength channels by sending the light to an array of (dispersive) waveguides, in this case photonic wires, with a fixed length difference between the array arms.^{2,11} For the central wavelength, the length difference is chosen such that the light in all arms arrives in phase at the output, refocusing the light back into the central waveguide. For other wavelengths, there will be a linear phase difference between the arms, resulting in a refocus point that is somewhat shifted with respect to the central waveguide.

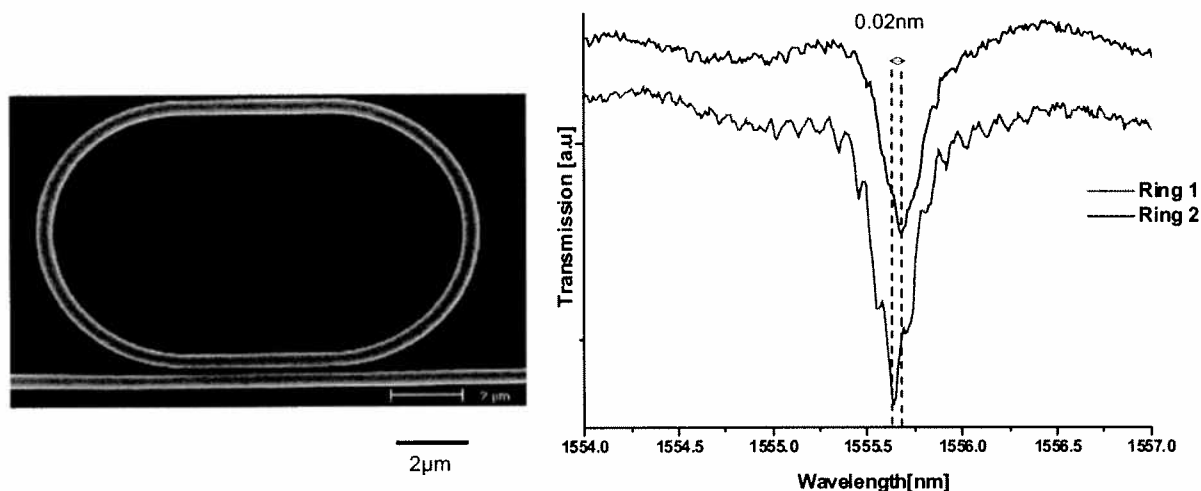


Figure 7. Racetrack resonator notch filter in silicon-on-insulator. Left: SEM micrograph. Right: transmission of two nominally identical rings separated 2 mm on the wafer.

In figure 8 an arrayed waveguide grating with 8 wavelength channels is shown. The delay length and the positions of the output waveguides were chosen to result in a channel spacing of 3.2 nm or 200 GHz . The crosstalk level between channels is -25 dB . The insertion loss of the device is only 1 dB for the central wavelength channel, down to 2.7 dB for the outer channels. This low insertion loss is due to the use of the low-contrast shallow etch in the star coupler regions. When waveguide light from a photonic wire is directly coupled to a slab waveguide, it has both a strong reflection, but also a very wide diffraction pattern, which would make aberration-free refocusing very difficult. Reducing the contrast and also broadening the waveguide results in very low reflections and a narrower diffraction pattern.

4.3 Planar concave echelle gratings

An alternative demultiplexer technique is to use a diffraction grating etched into the slab waveguide.¹² Such a device is shown in figure 9. Because simple etched facets have a limited reflectivity of about 30%, we have etched DBR gratings into the facets. This boosts the reflectivity to about 80%. Also, just as with the AWG, the insertion loss is reduced by using shallow waveguides for the aperture. The end result is an insertion loss of -1.9 dB for the center channels, with a crosstalk level better than -25 dB .

4.4 Fiber coupling

One of the difficulties with photonic wires in silicon is the coupling to the outside world. This can be understood easily by comparing the $10\text{ }\mu\text{m}$ mode diameter of a single-mode fiber with the submicron modes of a photonic wire. While a taper can expand the mode horizontally, vertical expansion is less straightforward. In addition, a horizontal mode converter also needs cumbersome facet polishing for high-efficiency coupling.

The processing using two etch steps allows us to include shallow-etched diffraction gratings in our waveguides. Using the right parameters, a detuned second-order diffraction grating can couple light from a broad ridge waveguide to a single-mode fiber.¹³ This is shown in figure 10. The coupling efficiency is also plotted. In its simplest form, the grating has a peak efficiency of 31%, with a 1 dB bandwidth of 35 nm . It is also tolerant to misalignment, both in the horizontal directions as in the vertical direction.

It is possible to increase the coupling efficiencies using additional processing. For instance, a bottom mirror can be added which enhances the upwards coupling through constructive interference of the reflected downward diffracted wave and upward diffracted wave.¹⁴ Alternatively, the use of a high-index overlay cladding can also

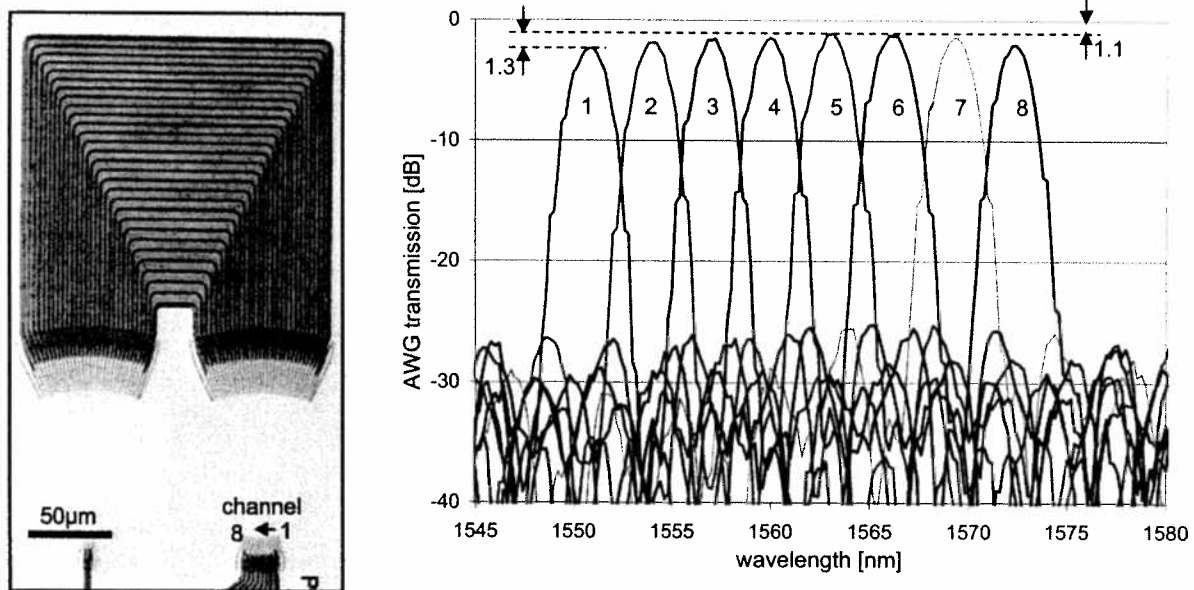


Figure 8. Arrayed waveguide grating in SOI. Left: The fabricated device. Right: transmission overlaid of the 8 output channels.

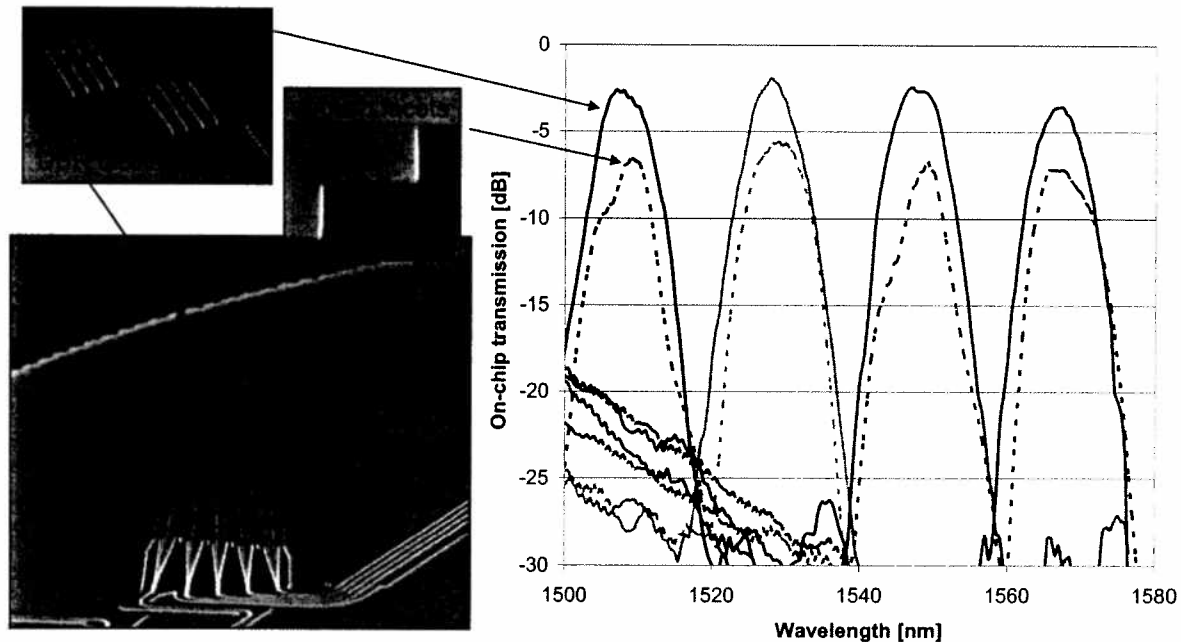


Figure 9. Planar concave echelle grating. Left: SEM micrographs, with a detail of the DBR facet. Right: transmission of the output channels.

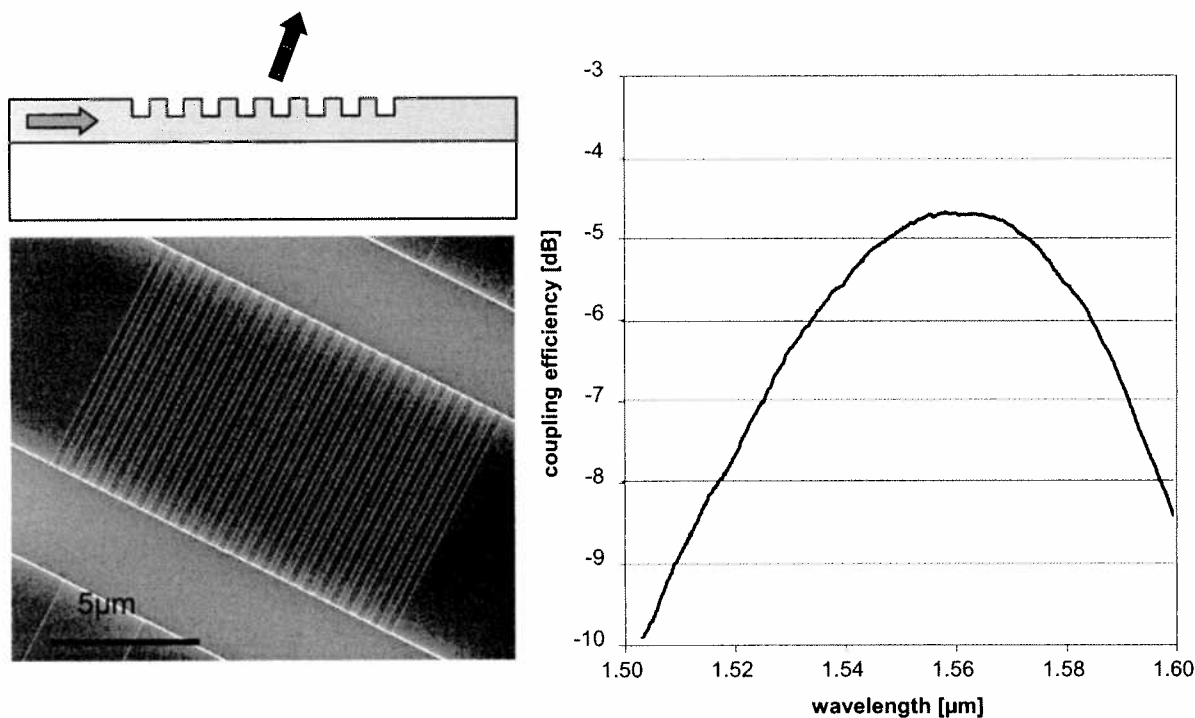


Figure 10. Fiber coupler grating. Left: the fabricated structure. Right: coupling efficiency as sunftion of wavelength.

boost the efficiency to over 80%.¹⁵ However, as these solutions came at an extra cost in terms of processing, they are only used in situations where the higher coupling efficiency is considered important.

Also, the fiber coupler grating only work for a single polarization, either TE or TM, depending on the grating parameters. However, by combining two 1-D gratings into a 2-D grating, any fiber polarization can be decomposed into the TE polarization in two separate waveguides.¹⁶ This allows a polarization-diversity approach.¹⁷

Still, the fiber coupler gratings couple the light to a $10\ \mu\text{m}$ wide waveguide. This can then be tapered down to a photonic wire. Adiabatically, these tapers are at least $150\ \mu\text{m}$ long. While complex spot-size converters based on multi-mode interferometry can be used, these are not easy to design and fabricate.¹⁸ However, one can also curve the grating, focusing the light directly in the nanophotonic waveguide.¹⁹

All of these techniques to improve fiber couplers, both in efficiency, polarization sensitivity and focusing, can be used together.

5. DEVICES AND APPLICATIONS

Their compact size, potential for large-scale integration and the possibilities of mass fabrication with CMOS technologies, make silicon photonic wire circuits very attractive for low-cost, high-volume applications. In this section, we will discuss three proof of principle implementations of photonic circuits for very different application fields: a wavelength duplexer for point-to-point access networks, a sensor film for strain, and a ultra-compact integrated 4-channel spectrometer with integrated photodetectors.

5.1 Example 1: a wavelength duplexer

As shown in section10, the grating fiber couplers have a high coupling efficiency only for a limited wavelength range. Actually, this wavelengths range corresponds to a certain angle of the fiber. In other words, for a different

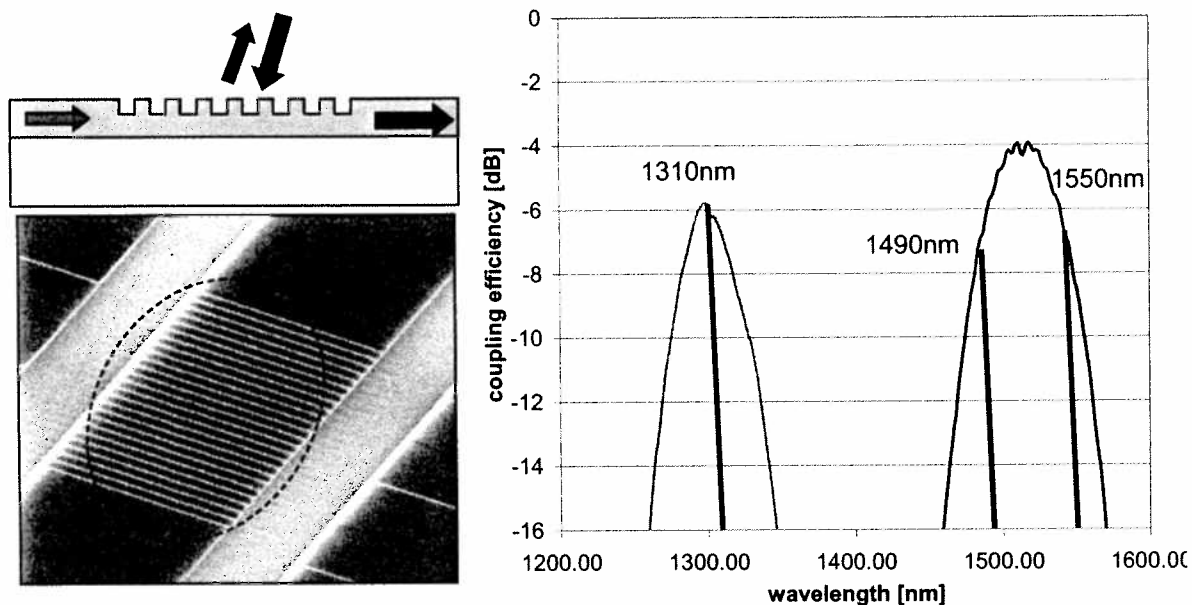


Figure 11. Grating-based duplexer. Light with wavelengths around $1.3 \mu\text{m}$ from the left waveguide is coupled to the fiber, while light from the fiber at $1.55 \mu\text{m}$ is coupled to the right waveguide.

fiber angle, the coupling wavelength range will shift. This allows to use the grating as a wavelength-splitting device. As shown in figure 11, depending on the wavelength, the light from the fiber is diffracted to either the right or the left waveguide. With the right grating parameters and for the right fiber angle, the wavelength splitting effect can be tuned to match the typical $1310 \text{ nm}/1550 \text{ nm}$ used for upstream/downstream in point-to-point fiber-to-the-home (FTTH) networks.²⁰

In figure 11 we plotted the transmission spectrum for upstream and downstream channels. We also indicated the upstream and downstream signal wavelengths. We see that the transmission curve for longer wavelengths seems to be somewhat detuned off the 1550 nm downstream wavelength. This is intentional, as it allows us to use an additional 1490 nm downstream wavelength for analog TV signals, with similar efficiency. In this example we used a simple grating coupler. Coupling efficiency can be greatly enhanced when using the different techniques discussed in section 4.4.¹⁵

5.2 Example 2: ring-based strain sensor

Silicon nanophotonic waveguides are very sensitive to variations in fabrication. But this, in turn, makes them ideally suited for sensors. After all, in a photonic wire, 25% of the light is confined in the waveguide cladding. This means that a ring resonator with a sufficiently high Q will have a sizeable shift of the resonance wavelength when the waveguide or its cladding is changed. This can be because of ambient factors like temperature, or by changing the composition of the cladding.²¹ Adding specific chemical ligands to the ring can even make it sensitive to the presence of specific chemical or biological compounds.^{10, 22}

The sensor device shown in figure 12 is designed to sense strain.²³ For its application, the sensor substrate is removed and the silicon circuit is transferred to a thin-film carrier, which can be attached to a structure. The three elongated racetrack resonators will respond with a different wavelength shift when stress is applied to the carrier. The rings elongated in the direction of the strain will experience the strongest wavelength shift. This allows us to measure strain in 2 dimensions, and even shear. This last property makes this strain sensor fairly unique compared to traditional strain sensors. The fourth, round ring is used to calibrate the sensor for other properties which affect the resonance wavelength, such as temperature. In figure 12 we can see the response of the four rings before and after strain is applied.

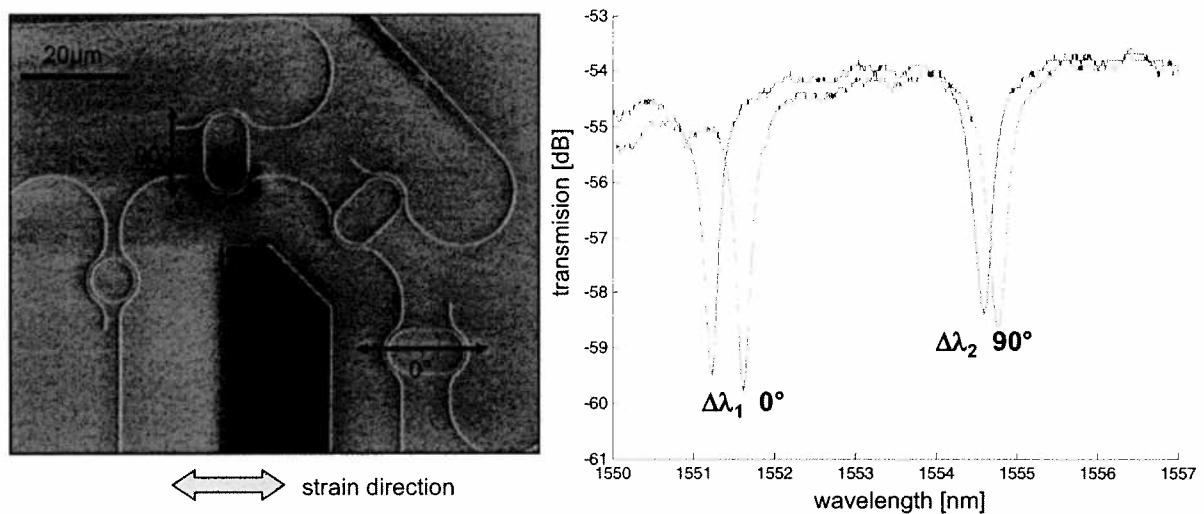


Figure 12. A strain sensor based on an SOI circuit with four ring resonators. Left: the fabricated device. Right: transmission of the circuit before and after the application of strain.

5.3 Example 3: An integrated photospectrometer

As a third application, we look at a concept for an integrated spectrometer.²⁴ In the device shown in figure 13 a circuit with a planar concave echelle grating is combined with integrated III-V photodetectors. Because silicon is not a good detector material around $1.55 \mu\text{m}$, we have used an adhesive bonding technique to integrate III-V metal-semiconductor-metal (MSM) photodetectors on the output waveguide of the demultiplexer.²⁵ These photodetectors have a very low dark current of 5 nA and a responsivity of 1 A/W at a wavelength of $1.55 \mu\text{m}$. The incoupling of light is done through a standard grating coupler, as discussed in section 4.4. The photocurrent of the detectors is plotted in figure 13. The number of channels of this spectrometer can easily be scaled by changing the parameters of the demultiplexer.²⁶

6. CONCLUSION

In this paper we have discussed the possibilities of integrated circuits based on silicon photonic wires. We have shown that low-loss wire waveguides allow for circuits with centimeter-scale interconnections and dense packing of waveguide elements, due to sharp bend radii. We also demonstrated a wide variety of wavelength-selective functions with good performance. For the interface with optical fibres we use grating fiber couplers, which allows us to couple light onto any place on the chip, and eradicates the need for cumbersome post-processing.

Finally, we applied these components into three case-studies for possible applications: a wavelength duplexer for FTTH point-to-point links, a ring-based strain sensor, and an integrated photospectrometer based on a planar concave echelle grating. These examples show that SOI nanophotonic circuits have unique properties that allow the miniaturization of real functional photonic ICs.

ACKNOWLEDGMENTS

W. Bogaerts acknowledges the Flemish Fund for Scientific Research (FWO) for a postdoctoral grant.

Part of this work was funded by the European Union in the framework of the IST network of Excellence ePIXnet and the FP6 project PICMOS. Part of this work was supported by the Belgian Science Policy through the IAP VI-10 project photonics@be.

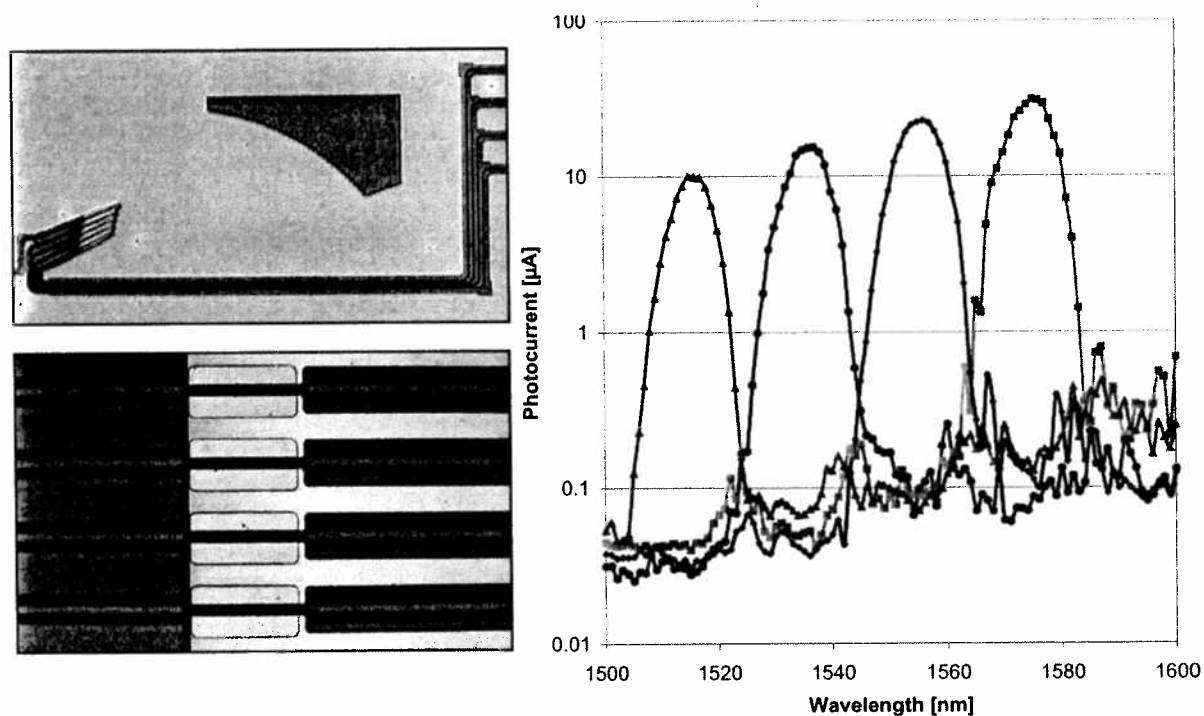


Figure 13. A 4-channel photospectrometer based on the planar concave grating from figure 9 with integrated photodetectors. Left: The demultiplexer and the integrated MSM photodetectors. Right: the photocurrent for the four photodetectors.

REFERENCES

- [1] Bogaerts, W., Baets, R., Dumon, P., Wiaux, V., Beckx, S., Taillaert, D., Luyssaert, B., Van Campenhout, J., Bienstman, P., and Van Thourhout, D., "Nanophotonic waveguides in Silicon-on-insulator fabricated with CMOS technology," *J. Lightwave Technol.* **23**(1), 401–412 (2005).
- [2] Bogaerts, W., Dumon, P., Van Thourhout, D., Taillaert, D., Jaenen, P., Wouters, J., S., B., Wiaux, V., and Baets, R., "Compact wavelength-selective functions in silicon-on-insulator photonic wires," *J. Sel. Top. Quantum Electron.* **12**, 1394–1401 (December 2006).
- [3] Dumon, P., Bogaerts, W., Wiaux, V., Wouters, J., Beckx, S., Van Campenhout, J., Taillaert, D., Luyssaert, B., Bienstman, P., Van Thourhout, D., and Baets, R., "Low-loss SOI photonic wires and ring resonators fabricated with deep UV lithography," *IEEE Photon. Technol. Lett.* **16**, 1328–1330 (May 2004).
- [4] Bogaerts, W., Wiaux, V., Taillaert, D., Beckx, S., Luyssaert, B., Bienstman, P., and Baets, R., "Fabrication of photonic crystals in Silicon-on-insulator using 248-nm deep UV lithography," *IEEE J. Sel. Top. Quantum Electron.* **8**(4), 928–934 (2002).
- [5] Bogaerts, W., Dumon, P., Van Thourhout, D., and Baets, R., "Low-loss, low-crosstalk crossings for soi nanophotonic waveguides," *Opt. Lett.* **32**, 2801–2803 (October 2007).
- [6] Selvaraja, S., Bogaerts, W., Van Thourhout, D., and Baets, R., "Fabrication of uniform photonic devices using 193nm optical lithography in silicon-on-insulator," *European Conference on Integrated Optics (ECIO)* (2008).
- [7] Selvaraja, S., Sleenckx, E., Bogaerts, W., Schaekers, M., Dumon, P., Van Thourhout, D., and Baets, R., "Low loss amorphous silicon photonic wire and ring resonator fabricated by cmos process," *European Conference on Optical Communication (ECOC)*, PD (2007).
- [8] Dulkeith, E., Xia, F., Schares, L., Green, W., and Vlasov, Y., "Group index and group velocity dispersion in silicon-on-insulator photonic wires," *Opt. Express* **14**, 3853–3863 (May 2006).

- [9] Gersen, H., Karle, T., Engelen, R., Bogaerts, W., Korterik, J., van Hulst, N., Krauss, T., and Kuipers, L., "Real-space observation of ultraslow light in photonic crystal waveguides," *Phys. Rev. Lett.* **94**, 073903 (February 2005).
- [10] De Vos, K., Bartolozzi, I., Schacht, E., Bienstman, P., and Baets, R., "Silicon-on-insulator microring resonator for sensitive and label-free biosensing," *Opt. Express* **15**(12), 7610–7615 (2007).
- [11] Dragone, C., "An NxN optical multiplexer using a planar arrangement of two star couplers," *IEEE Photon. Technol. Lett.* **3**, 812–814 (Sept. 1991).
- [12] Brouckaert, J., Bogaerts, W., Dumon, P., Van Thourhout, D., and Baets, R., "Planar concave grating demultiplexer fabricated on a nanophotonic silicon-on-insulator platform," *J. Lightwave Technol.* **25**(5), 1269–1275 (2007).
- [13] Taillaert, D., Bogaerts, W., Bienstman, P., Krauss, T., Van Daele, P., Moerman, I., Verstuyft, S., De Mesel, K., and Baets, R., "An out-of-plane grating coupler for efficient butt-coupling between compact planar waveguides and single-mode fibers," *J. Quantum Electron.* **38**(7), 949–955 (2002).
- [14] Van Laere, F., Roelkens, G., Ayre, M., Schrauwen, J., Taillaert, D., Van Thourhout, D., Krauss, T., and Baets, R., "Compact and highly efficient grating couplers between optical fiber and nanophotonic waveguides," *J. Lightwave Technol.* **25**, 151–156 (January 2007).
- [15] Roelkens, G., Vermeulen, D., Vand thourhout, D., and Baets, R., "High efficiency diffractive grating couplers for interfacing a single mode optical fiber with a nanophotonic silicon-on-insulator waveguide circuit," *Appl. Phys. Lett.* **92**(13), 131101 (2008).
- [16] Taillaert, D., Chong, H., Borel, P., Frandsen, L., De La Rue, R., and Baets, R., "A compact two-dimensional grating coupler used as a polarization splitter," *IEEE Photon Technol. Lett.* **15**(9), 1249–1251 (2003).
- [17] Bogaerts, W., Taillaert, D., Dumon, P., Van Thourhout, D., and Baets, R., "A polarization-diversity wavelength duplexer circuit in silicon-on-insulator photonic wires," *Opt. Express* **15**, 1567–1578 (February 2007).
- [18] Luyssaert, B., Vandersteegen, P., Taillaert, D., Dumon, P., Bogaerts, W., Bienstman, P., Van Thourhout, D., Wiaux, V., Beckx, S., and Baets, R., "A compact horizontal spot-size converter realized in silicon-on-insulator," *IEEE Photon. Technol. Lett.* **17**, 73–75 (January 2005).
- [19] Van Laere, F., Claes, T., Schrauwen, J., Scheerlinck, S., Bogaerts, W., Taillaert, D., O'Faolain, L., Van Thourhout, D., and Baets, R., "Compact focusing grating couplers for silicon-on-insulator integrated circuits," *Photon. Technol. Lett.* **19**(23), 1919–1921 (2007).
- [20] Roelkens, G., Van Thourhout, D., and Baets, R., "Silicon-on-insulator ultracompact duplexer based on a diffractive grating structure," *Opt. Express* **15**(16), 10091 (2007).
- [21] Debackere, P., Taillaert, D., Scheerlinck, S., De Vos, K., Bienstman, P., and Baets, R., "Si based waveguide and surface plasmon sensors," in [*Proc. SPIE*], *Photonics West* **6477**, p.647719 (2007).
- [22] De Vos, K., Bartolozzi, I., Taillaert, D., Bogaerts, W., Bienstman, P., Baets, R., and Schacht, E., "Optical biosensor based on silicon-on-insulator microring cavities for specific protein detection," *Proc. SPIE* **6447**, 6447DK–1 (January 2007).
- [23] Taillaert, D., Van Paepegem, W., Vlekken, J., and Baets, R., "A thin foil optical strain gage based on silicon-on-insulator microresonators," in [*Proc. SPIE*], *Third European Workshop on Optical Fibre Sensors (EWOFS)* **6619**, 661914 (2007).
- [24] Brouckaert, J., Roelkens, G., Selvaraja, S., Bogaerts, W., Dumon, P., Verstuyft, S., Van Thourhout, D., and Baets, R., "Compact silicon-on-insulator wavelength demultiplexer with heterogeneously integrated inalas/ingaas photodetectors," *European Conference on Optical Communication (ECOC)*, Tu.4.C.5 (2008).
- [25] Brouckaert, J., Roelkens, G., Van Thourhout, D., and Baets, R., "Compact inalas/ingaas metal-semiconductor-metal photodetectors integrated on silicon-on-insulator waveguides," *IEEE Photon. Technol. Lett.* **19**(19), 1484–1486 (2007).
- [26] Brouckaert, J., Bogaerts, W., Selvaraja, S., Dumon, P., Baets, R., and Van Thourhout, D., "Planar concave grating demultiplexer with high reflective bragg reflector facets," *Photon. Technol. Lett.* **20**(4), 309–311 (2008).

SEARCH PROCEEDINGS

Back to Title List
Monday 27 October 2008

[Search This Volume]

Search

Advanced Search

BROWSE PROCEEDINGS

- Proceedings
- By Year
- By Symposium
- By Volume No.
- By Volume Title
- By Technology

BROWSE JOURNALS

- Journals
- Optical Engineering
- J. Electronic Imaging
- J. Biomedical Optics
- J. Micro/Nanolithography, MEMS, and MOEMS
- J. Applied Remote Sensing
- J. Nanophotonics
- SPIE Letters Virtual Journal

SUBSCRIPTIONS & PRICING

- Institutions & Corporations
- Personal subscriptions

GENERAL INFORMATION

- About the Digital Library
- Terms of Use
- SPIE Home

PARTIAL TABLE OF CONTENTS

This volume is in progress. Newly published articles are added as they are completed and approved for publication.

Each article is designated by a unique six-digit article number. When citing these articles, the article number should be used instead of a page number; for example, Proc. SPIE 7134, 713402 (2008).

Volume 7134 -- Passive Components and Fiber-based Devices V

Ming-Jun Li, Ping Shum, Ian H. White, Xingkun Wu, Editors , November 2008

Conference Location: Hangzhou, China

Conference Date: 27 October 2008

- Photonic Crystal Fibers I
- Fiber Lasers and Amplifiers
- Optical Fibers I
- Fiber Bragg Gratings
- Best Student Papers
- Optical Components I
- Specialty Fibers
- Optical Components II
- Photonic Crystal Fibers II
- Optical Buffer and Signal Processing
- Optical Fibers II
- Silicon Photonics
- Nonlinear Signal Processing
- Optical Switches
- Polarization Effects
- Fiber Sensors
- Fiber Lasers
- Optical Devices
- Microstructured Fibers
- Fiber Ring Lasers
- Optical Filters
- Fiber Gratings
- Nonlinear Effects
- Poster Session

Click on the article number

Check Article(s) then ... Go

Adding to MyArticles will open a second window (Soltation login required).

YOUR CART

PHOTONIC CRYSTAL FIBERS I

Better photonic crystal fibres

J. C. Knight
Proc. SPIE Vol. **7134**, 713402 (Nov. 11, 2008)
Abstract Full Text: [PDF (737 kB)] (8 pages)

A novel design of highly negative dispersion photonic crystal fibers with central index dip

Honglei Li, Shuqin Lou, Tieying Guo, Hong Fang, Weiguo Chen, Liwen Wang, and Shuisheng Jian
Proc. SPIE Vol. **7134**, 713403 (Nov. 11, 2008)
Abstract Full Text: [PDF (221 kB)] (6 pages)

FIBER LASERS AND AMPLIFIERS

High-concentration erbium-doped fiber-based short cavity ring lasers

Lisong Liu, Yongjun Fu, Jian Peng, Kai Zheng, Xiangqiao Mao, Huai Wei, Fengping Yan, Honglei Lei, and Shuisheng Jian
Proc. SPIE Vol. **7134**, 713406 (Nov. 11, 2008)

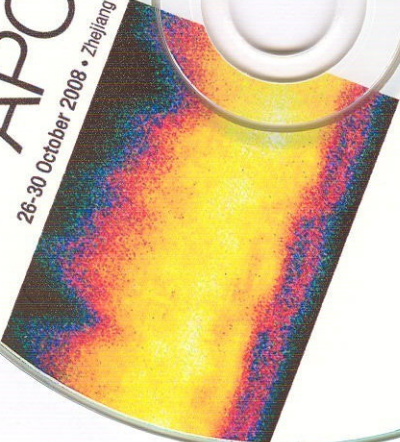
Technical Abstract Summary Digest


SPIE
APOC

26-30 October 2008 • Zhejiang International Conference Center • Hangzhou, China

Asia-Pacific
Optical Communications


Courtesy of Georgia Institute of Technology


SPIE
Chinese Optical Society (COS)
China Institute of Communications (CIC)
Joint Research Center of Photonics of the Royal Institute
of Technology (Sweden) and Zhejiang University (China)
© 2008 SPIE